引用格式：REN Xiaoping, WANG Hong. Propagation of Two-dimensional Surface Gap Solitons under Fractional Diffraction [J]. Acta Photonica Sinica, 2026, 55(2):0219002
任小平,王洪.分数阶衍射下两维表面带隙孤子的传输[J].光子学报,2026,55(2):0219002

分数阶衍射下两维表面带隙孤子的传输

任小平[1],王洪[2,3]
(1 山西财经大学 应用数学学院 太原 030006)
(2 华南理工大学 物理与光电学院 广东省光电工程技术研究开发中心,广州 510641)
(3 中山市华南理工大学现代产业技术研究院,中山 528437)

摘 要:聚焦分数阶衍射下两维表面带隙孤子的传输问题,采用数值计算方法,系统分析了自散焦Kerr非线性介质中位于大块介质与光学格子分界面处基本孤子和同相位偶极孤子的存在性、稳定性及传输特性。研究结果表明:表面带隙孤子可稳定存在于布洛赫第一带隙,且分界面处孤子呈现不对称形态。传输模拟和线性稳定分析的联合验证表明:除非分界面处的同相位偶极孤子在临近第一能带下边界的小区域内呈现不稳定外,其余表面带隙孤子在其整个存在区间保持稳定传输特性。当为表面带隙孤子引入相位倾斜因子时,较小的相位倾斜会引发孤子中心位置发生微小周期性震荡,但孤子的整体形态几乎无畸变;而较大的相位倾斜则会导致孤子中心位置产生无规律震荡,且其在传输过程中孤子逐渐失真。

关键词:表面带隙孤子;分数阶衍射;传输特性;非线性薛定谔方程;相位倾斜
中图分类号:O437 **文献标识码**:A **doi**:10.3788/gzxb20265502.0219002

0 引言

沿两种不同介质分界面传输的表面光波,因其在光传感、光转换及表面表征领域的潜在应用[1],近年来已成为研究热点并引起广泛关注。理论研究已证实,一维表面孤子可存在于非线性波导晶格的边缘[2];实验方面,研究者在AlGaAs波导阵列边缘成功观测到表面孤子,其结果与理论预测相吻合[3]。此后,一系列新型表面孤子相继报道,包括均匀介质与光学晶格分界面的表面带隙孤子[4]、两种不同光学晶格分界面的表面涡旋孤子[5]、非局域表面孤子[6]、一维啁啾光学格子中的表面缺陷孤子[7]以及空间调制非线性系统中的表面孤子[8]等。实验中亦观测到两维表面孤子的存在[9-10]。除此之外,含有增益损耗的光学格子与大块介质分界面也可以支持表面涡旋孤子的稳定传输[11]。然而,这些研究均基于标准薛定谔方程展开。

在量子力学领域,LASKIN N通过将费曼路径积分中的布朗轨迹替换为莱维轨迹以描述粒子演化行为,提出了广义的分数阶理论模型--分数阶薛定谔方程[12-14]。2015年,LONGHI S基于光束在非球面光学谐振器中的动力学特性,设计出可有效实现分数阶衍射效应的光学方案,构建了分数阶量子谐振腔的光学系统[15],由此开辟了“分数阶光场动力学”这一新兴研究方向。在光学领域,通过在傅里叶平面引入含有透射函数的相位掩模器可实现分数阶拉普拉斯算子。此后,光束在光学系统中的传输动力学特性逐步被揭示,包括“Z”形轨迹或漏斗状结构[16]、无衍射与锥形衍射现象[17]及周期性震荡行为[18-19]等。当分数阶衍射(色散)效应与非线性效应达到平衡时,分数阶薛定谔方程中可支撑多种形态孤子的存在,包括非局域孤子[20]、矢量孤子[21]、带隙孤子[22]、一维表面带隙孤子[23]、涡旋孤子[24-27]、基本孤子[28-31]、非对称孤子[32]与多峰孤子[33-34]等。同时,分数阶衍射调控下的对称破缺[35]、鬼态[36-37]、耦合孤子[38-39]也等特殊动力学现象也相继被揭示。近年来,学者们围绕分数阶非线性薛定谔方程展开了多维度研究,非均匀光纤中孤子的动力学行为[40]、变系

基金项目:山西省基础研究计划(202303021212167),广东省重点领域研发计划重大项目(2020B010171001),中山市科技发展专项资金(2023A4002)
第一作者:任小平,rxpcc2020@163.com
通讯作者:王洪,phhwang@scut.edu.cn
收稿日期:2025-09-01;**录用日期**:2025-12-01

数模型的解析解构造与调制不稳定性分析[41]、莫尔晶格中两维孤子的特性[42]、分数阶衍射对PT对称系统非线性相变的调控效应[43]以及对偶莱维指数条件下基本孤子与涡旋孤子的形成与传输[44]进一步完善了分数阶非线性薛定方程的理论体系，为光孤子在光通信、非线性光学器件等领域的应用奠定了基础。但目前关于分数阶衍射下两维表面带隙孤子的传输研究仍较匮乏，影响其传输的关键因素尚不明确。为此，本文重点研究布洛赫第一带隙中两维表面基本孤子与同相位偶极孤子的存在性和稳定性，并分析传播常数、莱维指数及相位倾斜等因素对孤子传输特性的调控作用。

1 理论模型

在傍轴近似下，光束在含分数阶衍射效应的大块介质与光学格子分界面处的传输行为，可由如下分数阶非线性薛定谔方程来描述：

$$\mathrm{i}\frac{\partial\psi}{\partial z}-\left(-\frac{\partial^2}{\partial x^2}-\frac{\partial^2}{\partial y^2}\right)^{\alpha/2}\psi+V(x,y)\psi-|\psi|^2\psi=0 \tag{1}$$

式中，$\psi(x,y,z)$为无量纲化的光场振幅包络，(x,y)和z分别是归一化的横向坐标与纵向坐标。$\left(-\frac{\partial^2}{\partial x^2}-\frac{\partial^2}{\partial y^2}\right)^{\alpha/2}$表示分数阶导数的拉普拉斯算符，该算符可通过傅里叶变换定义为[33]

$$\left(-\frac{\partial^2}{\partial x^2}-\frac{\partial^2}{\partial y^2}\right)^{\alpha/2}\psi(x,y)=F^{-1}\left\{\left(k_x^2+k_y^2\right)^{\alpha/2}F\left[\psi(x,y)\right]\right\} \tag{2}$$

式中，F和F^{-1}分别为傅里叶变换与傅里叶逆变换算子。α为莱维指数，满足$1<\alpha\leqslant 2$，用于表征分数阶衍射效应的强弱；当$\alpha=2$时，对应传统衍射效应，此时方程(1)退化为标准非线性薛定谔方程。在实验上，可以设计一个光学$4f$系统(由两个透镜组成，两个透镜的焦距均为f，两者之间的距离为$2f$)，在$4f$系统的频谱面(两个透镜中间)放置传输函数为$t(x)=\exp\left[-\mathrm{i}(\beta|x|^{\alpha})/2\right]$的相位掩模器，实现分数阶拉普拉斯算子的作用[15]。

$V(x,y)$是光学格子，可以表示为

$$V(x,y)=\begin{cases}V_0\left\{\cos^2\left[(x+y)/\sqrt{2}\right]+\cos^2\left[(x-y)/\sqrt{2}\right]\right\} & x\geqslant 0\\ 0 & x<0\end{cases} \tag{3}$$

式中，V_0为光学格子的势深。本文中固定$V_0=7$，对应的光学格子分布如图1(a)所示。

首先分析光学格子的能带结构。对于不含非线性项的方程(1)，其解可表示为

$$U=f(x,y)\exp(\mathrm{i}k_x x+\mathrm{i}k_y y)\exp(\mathrm{i}\mu z) \tag{4}$$

式中，$f(x,y)$是与光学格子周期一致的周期函数，k_x和k_y分别为x和y方向的布洛赫波，μ为传播常数。采用平面波展开法可求解得到光学格子的能带结构，其随莱维指数α的演化规律如图1(b)所示。由图1(b)可知，第一带隙与半无穷带隙随莱维指数的增大逐渐拓宽，而其它带隙则随莱维指数的增大逐渐收窄，与一维光学格子带隙随莱维指数的变化趋势[23]一致。

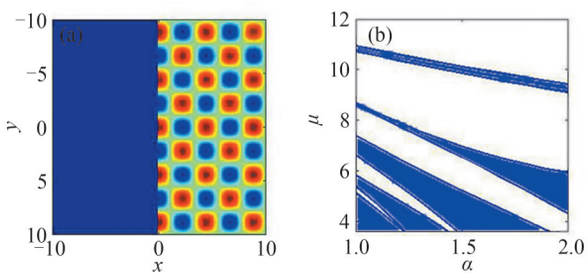


图1 光学格子和光学格子能带结构。(a)光学格子；(b)能带结构

Fig. 1 The optical lattice and band structure of the optical lattice. (a) The optical lattice; (b) Band structure of the optical lattice versus the Lévy index (blue regions represent bands, while white regions correspond to bandgaps)

其次，假设式(1)的解具有如下形式

$$\psi(x,y,z)=U(x,y)\exp(\mathrm{i}\mu z) \tag{5}$$

将式(5)带入式(1)可得

$$-\mu U-\left(-\frac{\partial^2}{\partial x^2}-\frac{\partial^2}{\partial y^2}\right)^{\alpha/2}U+VU-|U|^2U=0 \tag{6}$$

采用改进的平方算子法[45]可解得式(6)的数值解，其中$P=\int_{-\infty}^{+\infty}\int_{-\infty}^{+\infty}|U|^2\mathrm{d}x\mathrm{d}y$表示表面带隙孤子的功率。

为分析表面带隙孤子的线性稳定性，在形式解(式(5))中引入微扰，表达式为

$$\psi(x,y,z)=\exp(\mathrm{i}\mu z)\{U(x,y)+[p(x,y)-q(x,y)]\exp(\lambda z)+[p(x,y)+q(x,y)]^*\exp(\lambda^* z)\} \tag{7}$$

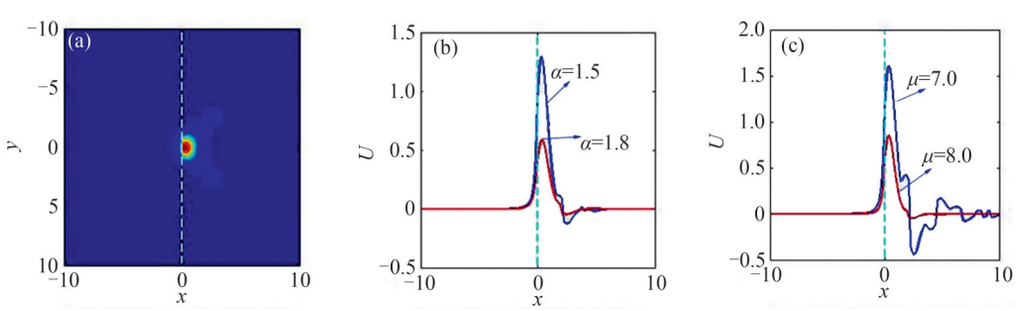
式中，$|p|\ll|U|$，$|q|\ll|U|$为扰动函数；“*”表示复共轭，λ为扰动增长率。将式(7)带入式(1)，可得

$$\begin{cases}\mathrm{i}\lambda p=-\mu q-\left(-\dfrac{\partial^2}{\partial x^2}-\dfrac{\partial^2}{\partial y^2}\right)^{\alpha/2}q+Vq+\gamma|\varphi|^2q\\ \mathrm{i}\lambda q=-\mu p-\left(-\dfrac{\partial^2}{\partial x^2}-\dfrac{\partial^2}{\partial y^2}\right)^{\alpha/2}p+Vp+3\gamma|\varphi|^2p\end{cases} \tag{8}$$

式(8)的数值解可以通过傅里叶配点法[46]得到。如果本征值的实部$\mathrm{Re}(\lambda)>0$，则表面带隙孤子是线性不稳定的；否则，表面带隙孤子线性稳定。

2 表面带隙孤子的强度分布

首先，分别对分界面与非分界面处的基本孤子及同相位偶极孤子展开研究，发现这些孤子均存在于第一带隙中。图2展示了这些表面带隙孤子的强度分布特征。由图2(a)～2(c)中分界面处基本孤子的强度分布及图2(e)、2(h)中分界面处同相位偶极孤子的强度分布可见：受分界面两侧介质不对称性的影响，孤子呈现不对称形态，且强度分布主要集中在光学格子一侧。这主要是因为在均匀介质中，单纯依靠介质的非线性效应平衡分数阶衍射效应，对光的束缚能力较弱。在光学格子中，束缚光孤子依靠的是非线性效应和光学格子共同平衡分数阶衍射效应，光学格子本身就提供了一个周期性的束缚结构，这个势场能够有效捕获和局域化光波，对光的束缚能力更强。在分界面，均匀介质一侧束缚能力弱，光学格子一侧束缚能力强，系统为了达到最终的稳定状态，会自发地将大部分光能量重新分布到束缚能力更强的光学格子一侧，从而在强度分布上呈现出明显的不对称性。此外，分界面处的同相位偶极孤子存在对称破缺现象，随着传播常数的增大，该偶极孤子逐渐退化为基本孤子，其强度分布与非分界面处基本孤子的形态一致。图2(b)及2(g)，2(h)，2(i)中的结果表明，孤子振幅随莱维指数的增大而减小，与一维系统中，孤子振幅随莱维指数的变化一致[23]；同时，孤子振幅也随传播常数的增大而减小(如图2(c)所示)。在第二能带的上边界附近(如$\mu=7$)表面带隙孤子的右侧衍生出明显的强度尾巴，呈现出显著的非对称特征，具体分布如图2(c)所示。



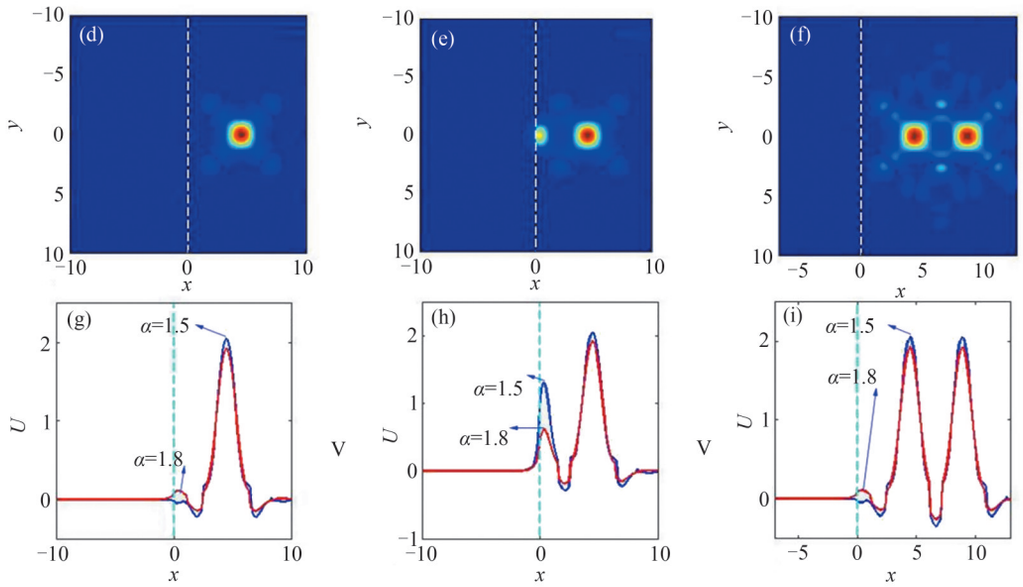


图2 表面带隙孤子的强度分布。(a)分界面处基本孤子;(b)分界面处基本孤子;(c)分界面处基本孤子;(d)非分界面处基本孤子;(e)分界面处同相位偶极孤子;(f)非分界面处同相位偶极孤子;(g)非分界面处基本孤子;(h)分界面处同相位偶极孤子;(i)非分界面处同相位偶极孤子

Fig. 2 Intensity profiles of surface gap solitons. (a) Fundamental solitons at the interface; (b) Fundamental solitons at the interface; (c) Fundamental solitons at the interface; (d) Fundamental solitons away from the interface; (e) In-phase dipole solitons at the interface; (f) In-phase dipole solitons away from the interface; (g) Fundamental solitons away from the interface; (h) In-phase dipole solitons at the interface; (i) In-phase dipole solitons away from the interface

3 表面带隙孤子的传输

3.1 孤子的稳定性分析

选取 $\alpha=1.5$, $V_0=7$ 进行分析。图3的结果显示:表面带隙孤子的功率随传播常数的增大呈单调递减趋势。其中,分界面处的基本孤子、同相位偶极孤子以及非分界面处的基本孤子可以在其整个存在区间内保持稳定,这与一维表面带隙孤子的特性一致[23];不同的是,本研究所观测到的分界面处的基本孤子其存在不需要功率阈值,而一维系统中基本孤子的存在需要一个非零的功率阈值[23]。非分界面处的同相位偶极孤子则除在第一能带下边界附近的小区域内不稳定外,在其余存在区间内均能稳定传输。

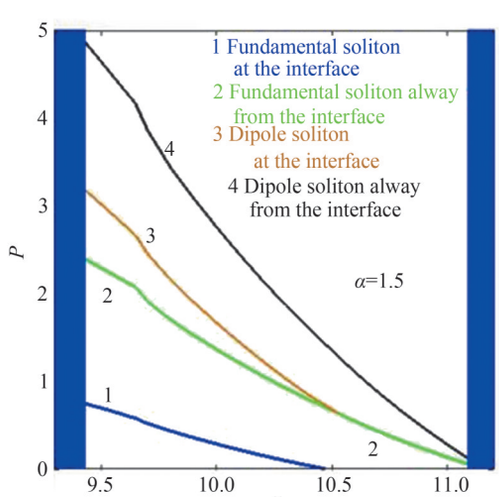


图3 表面带隙孤子功率随传播常数的变化。蓝色区域为布洛赫能带,红线表示孤子不稳定

Fig. 3 Power of surface solitons as a function of propagation constant. Blue shaded regions correspond to Bloch bands, and red line indicates the solitons are unstable

此外，还分析了 $\alpha=1.2$ 和 $\alpha=1.8$ 时表面带隙孤子的传输特性，发现其稳定规律与 $\alpha=1.5$ 时的情形完全一致。

为进一步验证表面带隙孤子的稳定性，在孤子中引入随机噪声（孤子振幅的5%），并采用分步傅里叶法模拟孤子的传输。选取 $\alpha=1.5$，$\mu=8.0$，其演化结果如图4所示。由图4(a)，4(e)，4(i)，4(m)和4(b)，4(f)，4(j)，4(n)可知，这些表面带隙孤子在传输过程中能够保持形态稳定；图4(c)，4(g)，4(k)，4(o)输入输出的对比结果则清晰显示，孤子的输出强度与输入强度分布完全一致。此外，图4(d)，4(h)，4(l)，4(p)的线性稳定谱表明，所有微扰特征值的实部均为零。这些结果共同证实了这些表面带隙孤子的稳定传输特性。

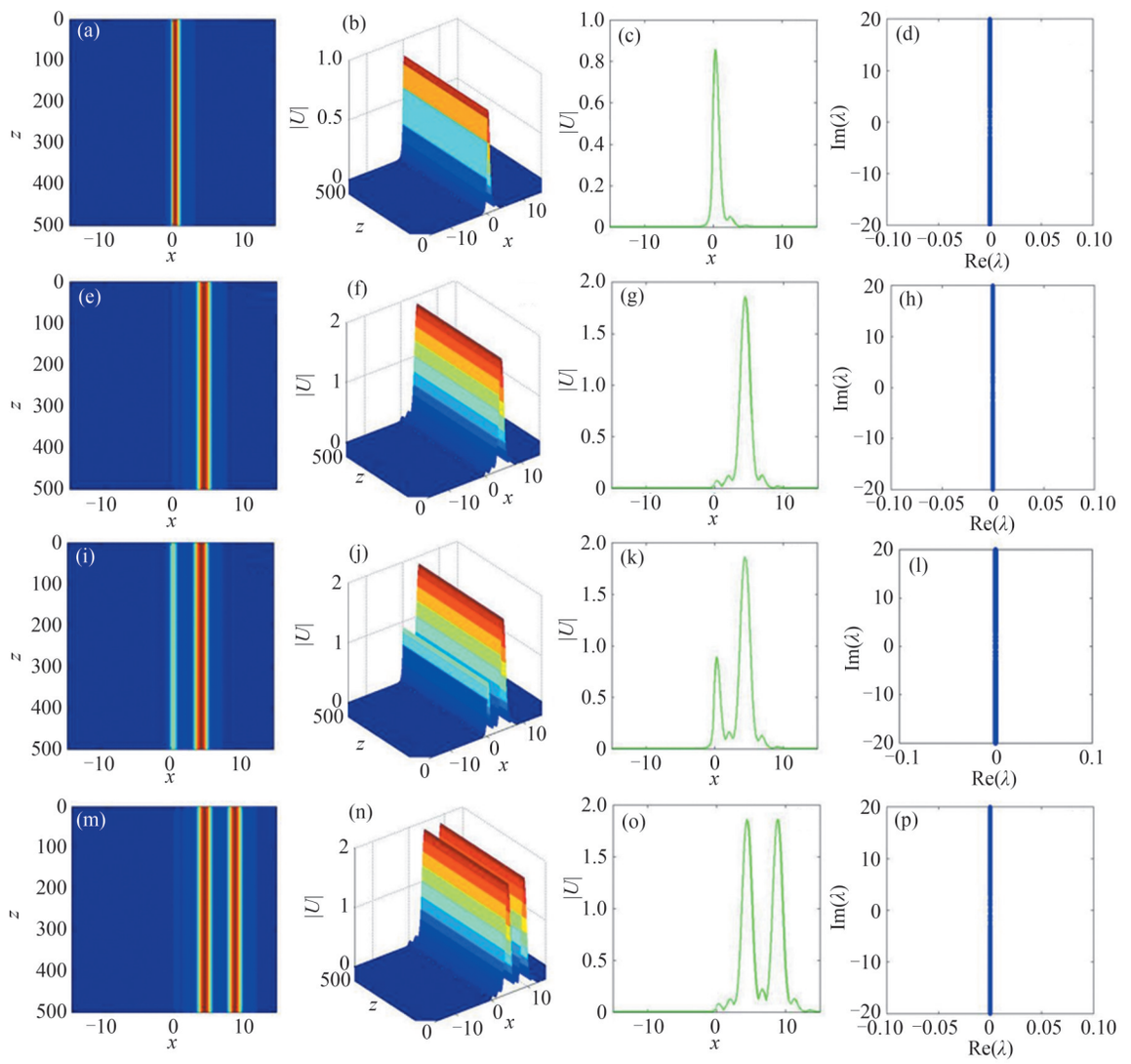


图4　$\alpha=1.5$，$\mu=8.0$ 时表面带隙孤子的传输。第一行、第二行、第三行和第四行分别对应分界面处基本孤子、非分界面处基本孤子、分界面处同相位偶极孤子和非分界面同相位偶极孤子。(a)，(e)，(i)，(m)传输剖面图；(b)，(f)，(j)，(n) 3D传输剖面图；(c)，(g)，(k)，(o)输入和输出强度剖面图；(d)，(h)，(l)，(p)线性稳定谱

Fig.4　Propagation of surface gap solitons with $\alpha=1.5$, $\mu=8.0$. The first row, second row, third row and last row correspond to fundamental solitons at the interface, fundamental solitons away from the interface, in-phase dipole solitons at the interface and in-phase dipole solitons away from the interface. (a), (e), (i) and (m) propagation profiles; (b), (f), (j) and (n) 3D propagation cross-profile; (c), (g), (k) and (o) Input and output cross profiles; (d), (h), (l) and (p) Linear stability spectrums

选取 $\alpha=1.5$，$\mu=9.8$，图5(a)和5(b)显示，非分界面的同相位偶极孤子传输至 $z=300$ 左右时，强度逐渐集中于单峰并呈现类呼吸子形态；孤子输入与输出的剖面图（图5(c)）进一步证实，其最终强度孤子的强度主要汇聚与单个峰。同时，对应的线性稳定谱（图5(d)）显示存在实部非零的微扰特征值，表明该孤子线性不稳定。

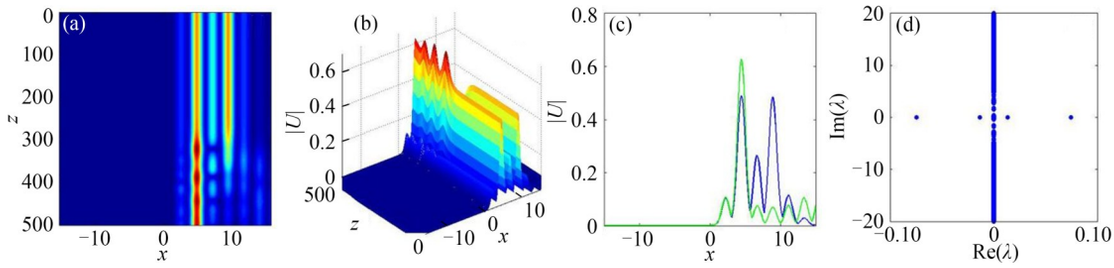


图5 不稳定区间内非分界面处同相位偶极孤子的传输($\alpha=1.5,\mu=9.8$)。(a)传输剖面图;(b)3D传输剖面图;(c)输入(蓝色线)和输出(绿色线)强度剖面图;(d)线性稳定谱

Fig. 5 Propagation of unstable in-phase dipole soliton away from the interface ($\alpha=1.5,\mu=9.8$). (a) Propagation profiles; (b) 3D propagation cross-profile; (c) Input (blue line) and output (green line) cross profiles; (d) Linear stability spectrums

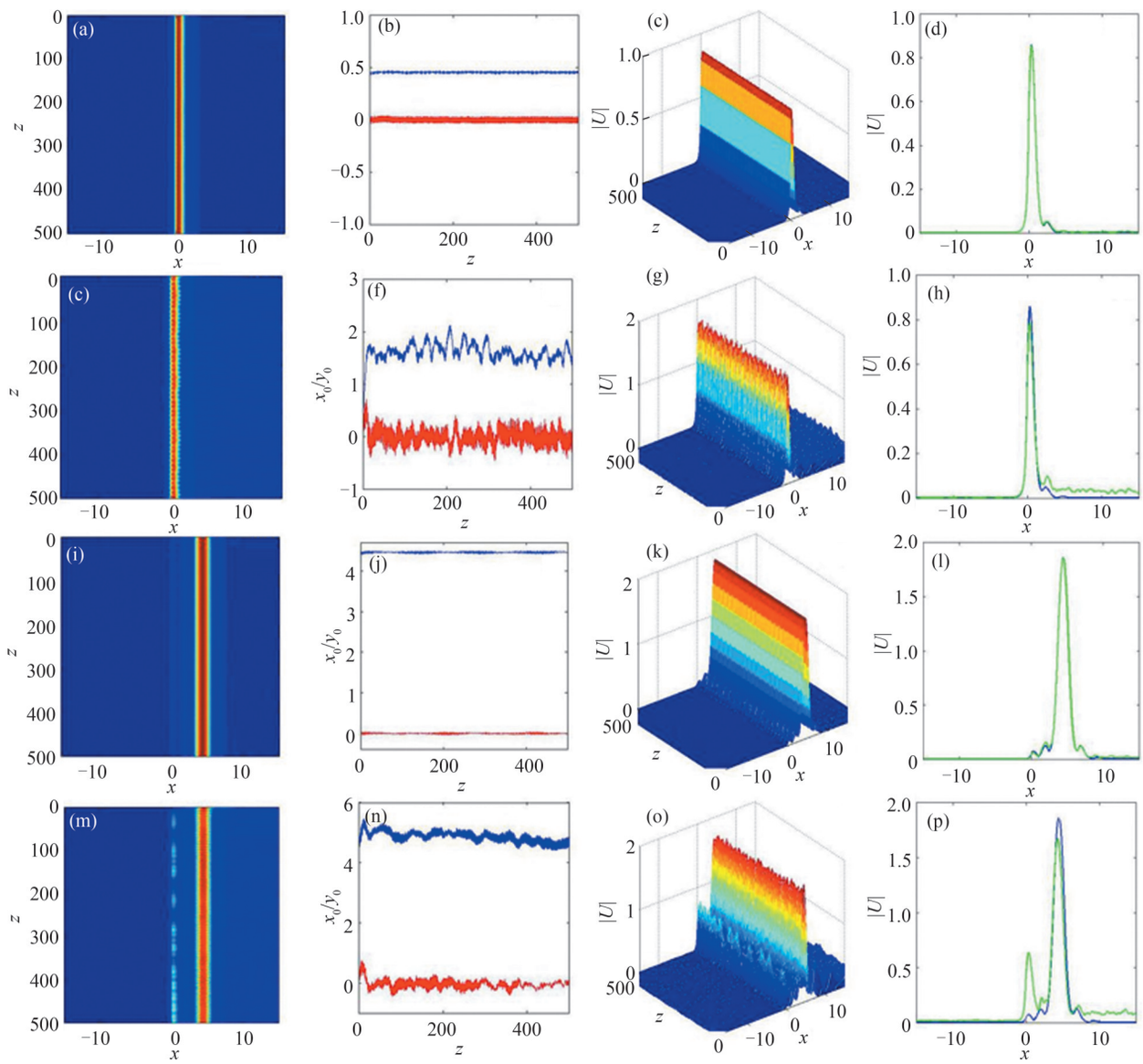


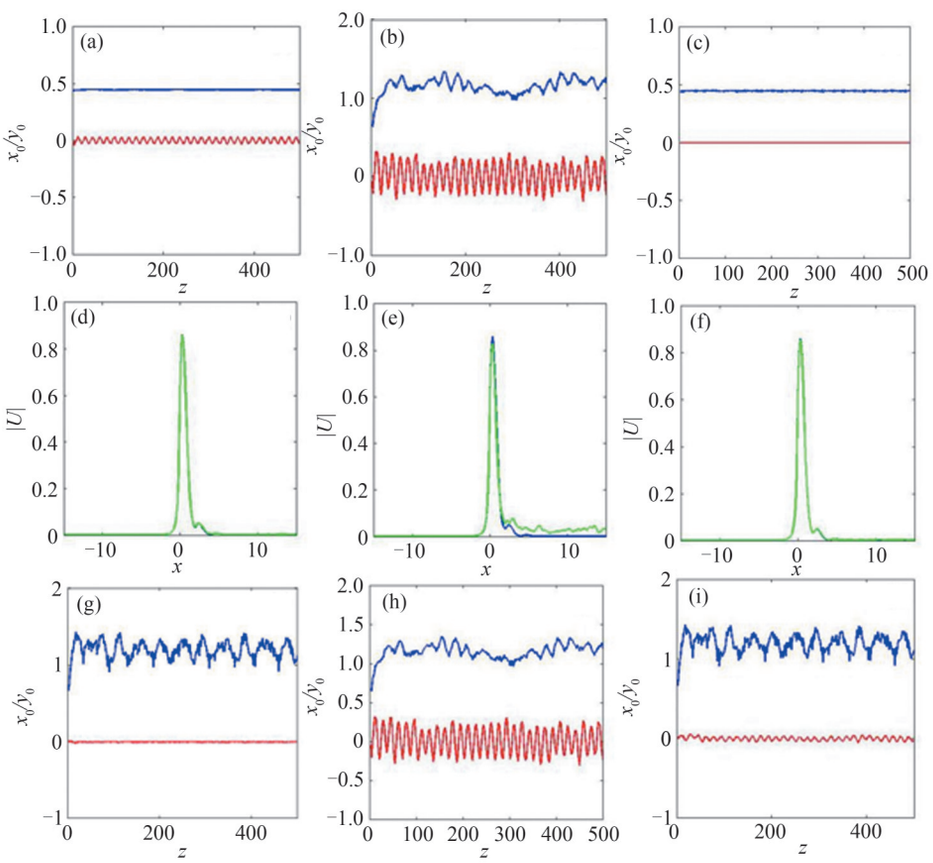
图6 相位倾斜对表面带隙孤子传输的影响。第一行($c=0.1$)和第二行($c=1$)对应分界面处基本孤子,第三行($c=0.1$)和第四行($c=1$)对应非分界面处基本孤子。(a),(e),(i),(m)传输剖面图;(b),(f),(j),(n)质心随传输距离的变化;(c),(g),(k),(o)3D传输剖面图;(d),(h),(l),(p)输入和输出强度剖面图

Fig.6 Influence of phase tilt on the the propagation characteristics of surface gap solitons. First row ($c=0.1$) and second row ($c=1$) correspond to fundamental solitons at the interface; third row ($c=0.1$) and last row ($c=1$) rows correspond to fundamental solitons away from the interface. (a), (e), (i) and (m) propagation profiles; (b), (f), (j) and (n) Mass center versus propagation distance; (c), (g), (k) and (o) 3D propagation cross-profile; (d), (h), (l) and (p) Input (blue lines) and output (green lines) cross profiles

3.2 相位倾斜对孤子传输的影响

以基本孤子为研究对象，进一步分析了相位倾斜对表面带隙孤子传输特性的影响。选取 $\alpha=1.5$，$\mu=8.0$，通过在基本孤子中引入相位倾斜因子 $\exp(\mathrm{i}cx+\mathrm{i}cy)$，并改变 c 的数值来探究其对孤子传输的调控规律。图 6(a)～6(d)（分界面处基本孤子）与 6(i)～6(l)（非分界面处基本孤子）的结果显示：在较小的相位倾斜（如 $c=0.1$）条件下，表面带隙孤子在传输过程中保持形态不变，但是中心位置会产生小振幅的周期性震荡。这里中心位置定义为 $(x_0,y_0)=\dfrac{1}{P}\displaystyle\int_{-\infty}^{+\infty}\int_{-\infty}^{+\infty}(x,y)|U|^2\mathrm{d}x\mathrm{d}y$，$P\neq 0$. 图 6(e)～6(h)（分界面处基本孤子）与 6(m)～6(p)（非分界面处基本孤子）则表明：当相位倾斜较大时，表面带隙孤子的中心位置出现无规律震荡，且形态在传输过程中逐渐失真。从三维传输剖面图（图 6(c)，6(g)，6(k)和 6(0)）及输入输出强度剖面图（图 6(d)，6(h)，6(l)和 6(p)）的对比可见：相位倾斜较小时，孤子形态传输过程中几乎不发生变化；而相位倾斜较大时，孤子形态发生显著畸变，这一现象在非分界面处的孤子中变现尤为明显。

此外，为了进一步分析相位倾斜对孤子传输的影响，以分界面处基本孤子为例，研究了相位倾斜因子为 $\exp(\mathrm{i}c_1x+\mathrm{i}c_2y)$ 时 $c_1\neq c_2$ 孤子的传输。鉴于 $c_1\neq c_2$ 时孤子的传输剖面图和三维传输剖面图与 $c_1=c_2$ 时的相似，这里只讨论孤子的中心变化以及输入与输出强度剖面图。$c_1=0$，$c_2=0.1$ 和 $c_1=0$，$c_2=1$ 时，孤子的中心变化如图 7(a)和 7(b)所示。易知，$c_1=0$，$c_2=0.1$ 时，即仅沿 y 方向增加一个较小的相位倾斜时，孤子的中心位置仅沿 y 方向发生振幅较小的周期震荡，而沿 x 方向几乎保持不变。当沿 y 分量增加的相位倾斜较大时，孤子的中心位置不仅沿 y 方向发生振幅较大的无规则震荡，而且沿 x 方向也会发生无规则变化。图 7(c)和 7(g)表明，仅沿 x 方向增加相位倾斜时，不管是较小的相位倾斜还是较大的相位倾斜，孤子的中心位置沿 y 方向都是几乎保持不变，这与仅沿 y 方向增加相位倾斜是不同的。当沿 x 方向增加一个较小的相位倾斜，沿 y 方向增加一个较大的相位倾斜时，孤子的中心变化与 $c_1=0$，$c_2=0.1$ 时的一致。图 7(h)和 7(i)表明当沿 y 方向增加一个较小的相位倾斜，沿 x 方向增加一个较大的相位倾斜时，孤子的中心位置沿 x 方向发生增幅较大的无规则震荡，而沿 y 方向发生振幅较小的周期性震荡。图 7(d)和 7(f)表明较小的相位倾斜几乎不改变孤子的形态。图 7(e)，7(g)，7(k)和 7(l)则表明，只要有一个方向的相位倾斜较大，都会引起孤子形态的改变，使其在传输中失真。



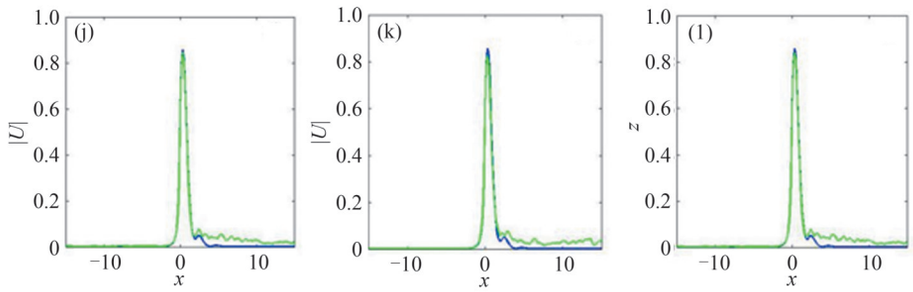


图7 $c_1 \neq c_2$时，相位倾斜对孤子传输的影响。第一行和第三行对应孤子质心随传输距离的变化，连线和红线分别对应x方向和y方向；第二行和第四行对应孤子输入和输出强度剖面图。(a)，(d)$c_1=0, c_2=0.1$；(b)，(e)$c_1=0, c_2=1$；(c)，(f)$c_1=0.1, c_2=0$；(g)，(j)$c_1=1, c_2=0$；(h)，(k)$c_1=0.1, c_2=1$；(i)，(l)$c_1=1, c_2=0.1$

Fig. 7 Influence of phase tilt on the the propagation characteristics of solitons with $c_1 \neq c_2$. The first row and third row correspond to mass center versus propagation distance, and the blue and red lines indicate the changes of the center along the x and y directions, respectively. The second row and last row correspond to input (blue line) and output (green line) cross profiles. (a), (d) $c_1=0, c_2=0.1$; (b), (e) $c_1=0, c_2=1$; (c), (f) $c_1=0.1, c_2=0$; (g), (j) $c_1=1, c_2=0$; (h), (k) $c_1=0.1, c_2=1$; (i), (l) $c_1=1, c_2=0.1$

3.3 莱维指数对孤子存在性与稳定性的影响

为进一步分析莱维指数对表面带隙孤子存在性与稳定性的调控作用，选择分界面处及非分界面处基本孤子为研究对象，探究了孤子存在区域与稳定区域随莱维指数的演化规律。图8的结果表明：表面带隙孤子的存在区间与稳定区间均随莱维指数的增大而逐渐拓宽。其中，分界面处的基本孤子(图8(a))在整个存在区间稳定，而非分界面处的基本孤子(图8(b))仅在小范围内不稳定，在大部分存在区域中均可稳定传输。

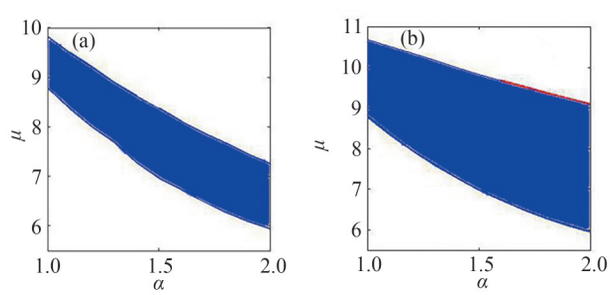


图8 表面基本孤子存在区域与稳定区域随莱维指数的变化。(a)分界面处基本孤子；(b)非分界面处基本孤子。阴影区域表示孤子的存在区间，其中蓝色阴影为稳定区域，红色阴影为不稳定区域

Fig. 8 Existence and stable regions of fundamental solitons as a function of Lévy index. (a) Fundamental solitons at the interface; (b) Fundamental solitons away from the interface. Shaded regions represent the existence ranges of solitons, where blue shaded areas correspond to stable regions and red shaded areas correspond to unstable regions

4 结论

本文系统研究了分数阶衍射下位于大块介质与光学格子分界面处的表面基本带隙孤子及同相位偶极带隙孤子的传输特性，并对比分析了分界面与非分界面处孤子的传输行为。研究结果表明：受分界面两侧介质不对称性的影响，分界面处的表面带隙孤子强度分布呈现显著不对称性。这些表面带隙孤子具有良好的传输稳定性——除非分界面处的同相位偶极孤子在小范围区间内不稳定外，其余孤子在传输过程中均能保持形态、强度不变。此外，随着莱维指数的增大，表面带隙孤子的存在区间与稳定区间均逐渐拓宽。

参考文献

[1] MIHALACHE D, BERTOLOTTI M, SIBILIA C. IV nonlinear wave propagation in planar structures [J]. Progress in Optics, 1989, 27: 227-313.

[2] MAKRIS K G, SUNTSOV S, CHRISTODOULIDES D N, et al. Discrete surface solitons [J]. Optics Letters, 2005, 30: 2466-2468.

[3] SUNTSOV S, MAKRIS K G, CHRISTODOULIDES D N, et al. Observation of discrete surface solitons [J]. Physical

Review Letters, 2006, 96: 063901.
[4] KARTASHOV Y V, VYSLOUKH V A, TORNER L. Surface gap solitons [J]. Physical Review Letters, 2006, 96: 073901.
[5] KARTASHOV Y V, EGOROV A A, VYSLOUKH V A, et al. Surface vortex solitons [J]. Optics Express, 2006, 14: 4049-4057.
[6] YE F, KARTASHOV Y V, TORNER L. Nonlocal surface dipoles and vortices [J]. Physical Review A, 2008, 77: 033829.
[7] XIE J, HE Y, WANG H. Surface defect gap solitons in one-dimensional chirped optical lattices [J]. Journal of the Optical Society of America B, 2010, 27: 484-487.
[8] LI X, YU R, ZHANG N. Surface solitons supported by PT-symmetric lattice with spatially modulated nonlinearity [J]. Journal of Nonlinear Optical Physics & Materials, 2017, 26: 1750001.
[9] WANG X, BEZRYADINA A, CHEN Z, et al. Observation of two-dimensional surface solitons [J]. Physical Review Letters, 2007, 98: 123903.
[10] SZAMEIT A, KARTASHOV Y V, DREISOW F, et al. Observation of two-dimensional surface solitons in asymmetric waveguide arrays [J]. Physical Review Letters, 2007, 98: 173903.
[11] LI H, ZHU X, SHI Z, et al. Bulk vortices and half-vortex surface modes in parity-time-symmetric media [J]. Physical Review A, 2014, 89: 053811.
[12] LASKIN N. Fractional quantum mechanics and Lévy path integrals [J]. Physical Letters A, 2000, 268: 298-305.
[13] LASKIN N. Fractional quantum mechanics [J]. Physical Review E, 2000, 62: 3135-3145.
[14] LASKIN N. Fractional Schrödinger Equation [J]. Physical Review E, 2002, 66: 056108.
[15] LONGHI S. Fractional Schrödinger equation in optics [J]. Optics Letters, 2015, 40: 1117-1120.
[16] ZHANG Y, LIU X, BELIĆ M R, et al. Propagation dynamics of a light beam in a fractional Schrödinger equation [J]. Physical Review Letters, 2015, 115: 180403.
[17] ZHANG Y, ZHONG H, BELIĆ M R, et al. Diffraction-free beams in fractional Schrödinger equation [J]. Scientific Reports, 2016, 6(1): 23645.
[18] ZHANG F, WANG Y, LI L. Dynamics of Gaussian beam modeled by fractional Schrödinger equation with a variable coefficient [J]. Optics Express, 2018, 26: 23740-23750.
[19] WANG X, SONG L, LI L. Propagation of Gaussian beam based on two-dimensional fractional Schrödinger equation [J]. Optics Communications, 2021, 480: 126483.
[20] DONG L, HUANG C, QI W. Nonlocal solitons in fractional dimensions [J]. Optics Letters, 2019, 44: 4917-4920.
[21] XIE J, ZHU X, HE Y. Vector solitons in nonlinear fractional Schrödinger equations with parity-time-symmetric optical lattices [J]. Nonlinear Dynamics, 2019, 97: 1287-1294.
[22] HUANG C, DONG L. Gap solitons in the nonlinear Schrödinger equation with an optical lattice [J]. Optics Letters, 2016, 41: 5636-5639.
[23] XIAO J, TIAN Z, HUANG C, et al. Surface gap solitons in a nonlinear Schrödinger equation [J]. Optics Express, 2018, 26: 2650-2658.
[24] YAO X, LIU X. off-site and on-site vortex solitons in space-fractional photonic lattices [J]. Optics Letters, 2018, 43: 5749-5752.
[25] DONG L, HUANG C. Vortex solitons in fractional systems with partially parity-time-symmetric azimuthal potentials [J]. Nonlinear Dynamics, 2019, 98: 1019-1028.
[26] MALOMED B A. Optical solitons and vortices in fractional media: a mini-review of recent results [J]. Photonics, 2021, 8: 353.
[27] YAN L, ZHANG D, ZHU H. Stable fractional vortex solitons in a ring potential [J]. Chaos Solitons and Fractals, 2025, 191: 115858.
[28] REN X, DENG F, HUANG J. Families of fundamental solitons in the two-dimensional superlattices based on the fractional Schrödinger equation [J]. Optics Communications, 2022, 519: 128439.
[29] ZENG L, ZENG J. One-dimensional solitons in fractional Schrödinger equation with a spatially modulated nonlinearity: nonlinear lattice [J]. Optics Letters, 2019, 44: 2661-2664.
[30] YAO X, LIU X. Solitons in the fractional Schrödinger equation with parity-time-symmetric lattice potential[J]. Photonics Research, 2018, 6: 875-879.
[31] ZENG L, MIHALACHE D, MALOMED B A, et al. Families of fundamental and multipole solitons in a cubic-quintic nonlinear lattice in fractional dimension [J]. Chaos, Solitons and Fractals, 2021, 144: 110589.
[32] ZHOU S, ZENG J, QIN Y, et al. Asymmetric localized states at a nonlinear interface of fractional systems with optical lattices [J]. Frontiers in Physics, 2023, 10: 1116344.
[33] ZHU X, YANG F, CAO S, et al. Multipole gap solitons in fractional Schrödinger equation with parity-time-symmetric

optical lattices [J]. Optics Express, 2020, 28: 1631-1639.
[34] ZHU X, BELIĆ M R, MIHALACHE D, et al. Centrosymmetric multipole solitons with fractional-order diffraction in two-dimensional parity-time-symmetric optical lattices [J]. Physica D-Nonlinear Phenomena, 2024, 470: 134379.
[35] LI P, LI R, DAI C. Existence, symmetry breaking bifurcation and stability of two-dimensional optical solitons supported by fractional diffraction [J]. Optics Express, 2021, 29: 3193.
[36] ZHONG M. Two-dimensional fractional PPT-symmetric cubic-quintic NLS equation: Double-loop symmetry breaking bifurcations, ghost states and dynamics [J]. Physica D-Nonlinear Phenomena, 2023, 448: 133727.
[37] ZHONG M, YAN Z. Spontaneous symmetry breaking and ghost states in two-dimensional fractional nonlinear media with non-Hermitian potential [J]. Communications Physics, 2023, 6: 92.
[38] ZENG L, BELIĆ M R, MIHALACHE D, et al. Solitons in a coupled system of fractional nonlinear Schrödinger equations [J]. Physica D-Nonlinear Phenomena, 2023, 456: 133924.
[39] LI S R, BAO Y Y, LIU Y H, et al. Bright solitons in fractional coupler with spatially periodical modulated nonlinearity [J]. Chaos, Solitons and Fractals, 2022, 162: 112484.
[40] LIU M, WANG H, YANG H, et al. Study on propagation properties of fractional soliton in the inhomogeneous fiber with higher-order effects [J]. Nonlinear Dynamics, 2024, 112: 1327-1337.
[41] ROSHID M M, RAHMAN M M. Bifurcation analysis, modulation instability and optical soliton solutions and their wave propagation insights to the variable coefficient nonlinear Schrödinger equation with Kerr law nonlinearity [J]. Nonlinear Dynamics, 2024, 112: 16355-16377.
[42] LIU X, ZENG J. Two-dimensional localized modes in nonlinear systems with linear nonlocality and moiré lattices [J]. Frontiers of Physics, 2024, 19: 42201.
[43] HE X, ZHANG M, LI P, et al. Effects of fractional diffraction on nonlinear PT phase transitions and stability of dark solitons and vortices [J]. Optics Express, 2025, 33: 9369-9382.
[44] ZHONG M, CHEN Y, YAN Z, et al. Formation and propagation of fundamental and vortex soliton families in 1D and 2D dual-Lévy-index fractional nonlinear Schrödinger equations with cubic-quintic nonlinearity [J]. Physica D-Nonlinear Phenomena, 2024, 462: 134157.
[45] YANG J, LAKOBA T I. Universally-convergent squared-operator iteration methods for solitary waves in general nonlinear wave equations [J]. Studies in Applied Mathematics, 2017, 118: 153 - 197.
[46] YANG Jianke. Nonlinear waves in integrable and nonintegrable systems [M]. Philadelphia: SIAM, 2010.
杨建科.可积与不可积系统中的非线性波[M].费城:工业与应用数学学会出版社,2010.

Propagation of Two-dimensional Surface Gap Solitons under Fractional Diffraction

REN Xiaoping[1], WANG Hong[2,3]

(1 *School of Applied Mathematics, Shanxi University of Finance and Economics, Taiyuan* 030006, *China*)

(2 *Engineering Research Centre for Optoelectronics of Guangdong Province, School of Physics and Optoelectronics, South China University of Technology, Guangzhou* 510641, *China*)

(3 *Zhongshan Institute of Modern Industrial Technology, South China University of Technology, Zhongshan* 528437, *China*)

Abstract: Surface waves propagating along the interface of two distinct media have garnered significant attention in recent years, owing to their promising applications in fields such as optical sensing, optical switching, and surface characterization. Extensive research has been conducted on surface solitons based on the standard Schrödinger equation, and many novel characteristics have been found.

Recently, an extended version of the standard Schrödinger equation has been introduced into the system, where the diffraction term is described by a fractional-order derivative rather than the second-order derivative in the conventional form. This extended equation is referred to as the fractional Schrödinger equation. Promptly thereafter, an optical realization of the equation was proposed based on the transverse light dynamics in an aspherical optical resonator, alongside a scheme for generating dual-Airy states. Notably, this marked the first introduction of the fractional Schrödinger equation into the field of optics, which opened up a novel research direction in optics. Since then, numerous studies on solitons with fractional diffraction have been reported. However, relevant research on surface solitons supported by the

fractional nonlinear Schrödinger equation remains relatively scarce. Focusing on the propagation of two-dimensional surface gap solitons under fractional diffraction, this study investigates the existence, stability, and propagation properties of fundamental and in-phase dipole solitons at the interface between bulk media and an optical lattice in self-defocusing Kerr nonlinear media via numerical methods.

The band structure of the optical lattice was calculated via the plane-wave expansion method. Subsequently, the existence region of surface gap solitons was obtained by modified squared operator iteration method, while their stability was analyzed through the Fourier collocation method and further verified via the split-step Fourier method.

The results show that the first bandgap and the semi-infinite bandgap gradually broaden with an increase in the Lévy index, while the other bandgaps progressively narrow as the Lévy index increases. Both fundamental and in-phase dipole solitons can exist within the first gap of the Bloch bands, and both fundamental and in-phase dipole solitons at the interface exhibit an asymmetric morphology. As the Lévy index increases, the peak intensity of the soliton decreases. Similarly, the peak intensity also declines with an increase in the propagation constant. Combined verification through propagation simulations and linear stability analysis reveals that: except for the in-phase dipole solitons away from the interface, which exhibit instability in a small region near the lower edge of the first Bloch band, all other surface gap solitons maintain stability throughout their entire existence range. Additionally, it also indicates that as the Lévy index increases, both the existence interval and stability interval of surface gap solitons gradually broaden. When a phase tilt factor is introduced to the surface gap solitons, applying the phase tilt in a single direction yields distinct behaviors: a small phase tilt causes the soliton center to oscillate periodically only along the direction of the applied phase tilt. A large phase tilt in the y-direction not only induces irregular oscillations of the soliton center along the y-direction but also elicits such oscillations along the x-direction. However, a large phase tilt in the x-direction solely results in irregular oscillations of the soliton center along the x-direction. If the same phase tilt is introduced in both directions, a small phase tilt causes the soliton center to undergo periodic oscillations in both directions, while a large phase tilt leads the soliton center to exhibit irregular oscillations in both directions. The results indicate that a small phase tilt induces slight periodic oscillations in the soliton′s mass center, while the soliton shape remains nearly unchanged. In contrast, a large phase tilt leads to irregular oscillations in the mass center, accompanied by gradual distortion of the soliton.

Key words: Surface gap solitons; Fractional diffraction; Propagation characteristics; Nonlinear fractional Schrödinger equation; Phase tilt

OCIS Codes: 190.6135; 060.4510; 000.4430

CSTR: 32255.14.gzxb20265502.0219002

Foundation item: Fundamental Research Program of Shanxi Province (202303021212167), Science and Technology Plan Project of Guangdong Province (2020B010171001), Science and Technology Development Special Fund Projects of Zhongshan City (2023A4002)